RSJ2022AC2J2-01

# Design of 3-dof 2-link inflatable collaborative robot arm with internal drop stitch structure

*Gangadhara Naga Sai Gubbala, Masato Nagashima, Hiroki Mori(Waseda U), Young ah Seong(Hosei U), Hiroki Sato(Miyagi U), Ryuma Niiyama(Meiji U), Tetsuya Ogata(Waseda U)

## 1. Introduction

Physical interactions of robots with humans and surroundings are inevitable for a collaborative working environment. In our opinion, robots made from air-filled balloon structures are suitable for physical interactions with humans and the environment, which are known as Inflatable robots. Inflatable robots are lightweight and made of inherent compliant materials, hence are suitable for physical interactions with humans and the environment. Because of their lightweight and inclusion of dispersed structural and surface compliance in their design, inflatable robots can increase inherent safety qualities[1]. In case of unintended collisions with humans or surroundings, inflatable robots exert low force due to less effective inertia.

One of the problems with such robots is their inflatable structure is too compliant to perform work. The inherent soft structure of inflatable robots makes them susceptible to deformation due to dynamic forces and their weight. To overcome this, we introduce an internal drop-stitch structure for robustness. Inflatable bodies with internal drop-stitch are common in several applications such as surfing boards, boats, mattresses and camping houses.

In this work, we construct a 2-link inflatable robot with an internal drop stitch structure for stability. We conduct experiments on an inflatable arm with 1 Degree of Freedom (DOF) to investigate its physical properties. Based on these properties we finally design the 3DOF robot.

## 2. Related Work

Initial implementation of inflatable links in robotics has shown potential in various applications. In a design proposed by Suzumori et al. [2], they utilize helium filled balloon bodies and thin pneumatic muscles to inspect unreachable regions. Sanan et al. [3] investigated unintended physical human-robot interaction with an inflatable manipulator made from a polyurethane film. The Inflatable Humanoid Robot named King Louie is a complete end-to-end inflatable robot that is controlled by pneumatic segments using Linear Quadratic Regulator and Model Predictive Control [4]. Fabric-based spherical robot arm with 2 links 2 rotational degrees of freedom showcased a pres-sure-controlled inflatable robot arm [5].

The above-mentioned references showcase balloon-like structures without any internal reinforcement, whereas the following references showcase additional internal structures for enhancing the rigidity of inflatable bodies. Disney research was able to design a hybrid structure. The 6 DOF arm has two air-filled force sensing modules that passively absorb impact and provide contact force feedback. The arm has an inflated outer cover that encloses underlying mechanisms and force sensing modules [6].

Fig. 1: Transparent balloon sample to visualize drop stitch structure.

POIMO (POrtable and Inflatable MObility devices) built by Sato et al. [7] that comprises inflatable frames, wheels, and steering mechanisms that are made with an internal drop stitch structure. They outlined the fundamental mechanism and material characteristics of inflated constructions capable of supporting a human while also allowing for gentle deformations. We have utilized similar fabrication methods of POIMO for inflatable arm links. POIMO research focuses on understanding the deformation of the inflatable body upon static load applied to support the human on the mobility device.

## 3. Concept and Design of Inflatable Link

Figure 1 shows an inflatable body made of two cloth fabric materials connected by threads or space yarn. The yarn connecting the top layer with the bottom layer enables the Polyester stitches to hold the fabrics together. An inflatable body with high air pressure prevents them from bending, leaning, or tilting. The balloon structure is enclosed with the help of TPU (Thermoplastic Polyurethane) coating over the base cloth.

The design of an inflatable robot arm consists of primarily the shape of the link and the connection mechanism to another link or an actuator. As shown in figure 2, we have selected a simple cuboidal structure. We considered the cuboidal structure since we want to examine the properties of the inflatable arm

Fig. 2: Balloon sample compared to vernier caliper. Balloon size is close to a cuboid with a size of 950mm*150mm*150mm.

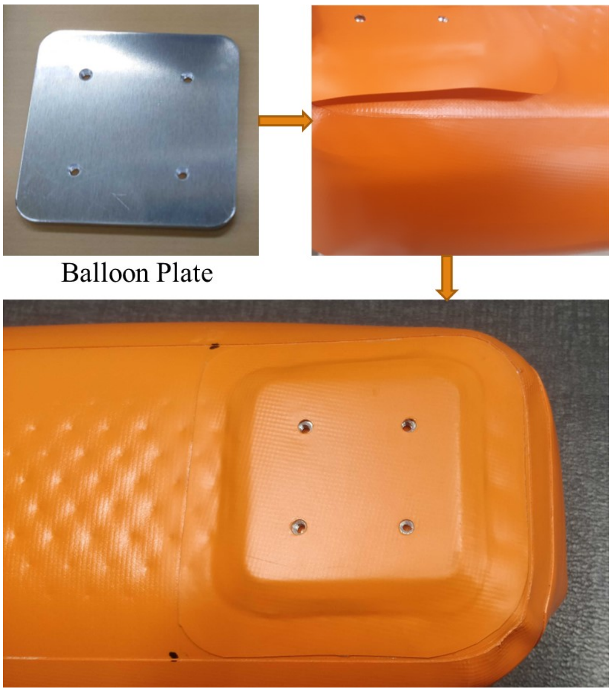


Fig. 3: The balloon plate is attached to the surface of the balloon with help of an adhesive.

in a cantilever position, with one side fixed and the other carrying a payload.

The connection from one link to another is made using a metal plate embedded within the balloon surface. The plate is of simple design with 4 M4 screw holes. As shown in figure 3, the balloon plate is attached to the surface of the balloon with fabric using adhesive. We designed a mediator plate that can connect the balloon plate and the servo frame to connect to a servomotor as shown in figure 4.

Based on previous connections, we can observe 2 possible link connections with a servo in between. We define 2 kinds of connections from figure 5a as End-to-End connection, Figure 5b can be defined as a Side-to-Side connection.

## 4. Experiments

### 4·1 Stationary Experiment

The stationary experiment is performed to analyze the inflatable body in the cantilever position. As

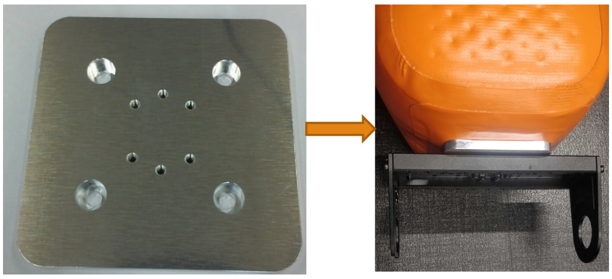

Fig. 4: Mediator plate connection to servo frame.

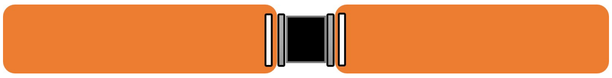

(a) End-to-End

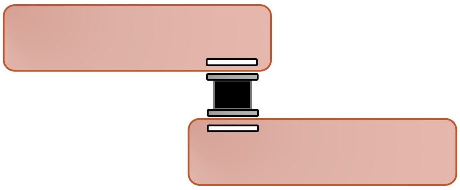

(b) Side-to-Side

Fig. 5: Possible balloon plate connection designs with 2 links. White and Grey represent balloon and mediator plates.

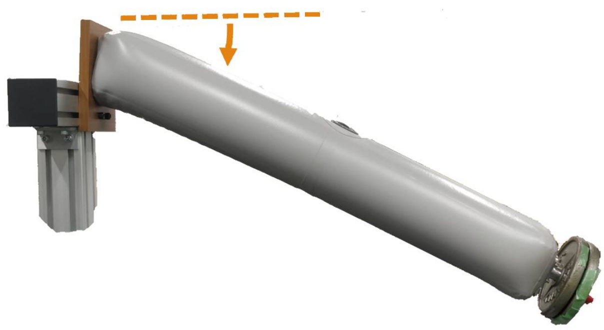

Fig. 6: Stationary experiment is implemented by measuring deformation angle from the horizontal reference line.

shown in figure 6, the deformation angle is calculated from a horizontal reference line for weights varying from 0kg to 2.5kg, 3.5kg, and 5.0kg, further after-effects are assessed with 0kg. The above process is repeated for 3 different combinations of fixed Parts of a balloon link and pay-load positions.

We define 3 kinds of connections concerning the number of plates and their positions on balloons. Figure 7 shows balloons with two plates. We examine the different combinations of payload and joint positions.

As shown in Figure 8, we can observe that the Side-Side design (c) has shown the least deformation. However, as shown in Figure 9, the Top-bottom design could recover the shape after the experiment while the Side-Side design (c) has not completely recovered and sustained plastic deformation. Hence, we select the top-bottom design as it showed better elastic properties.

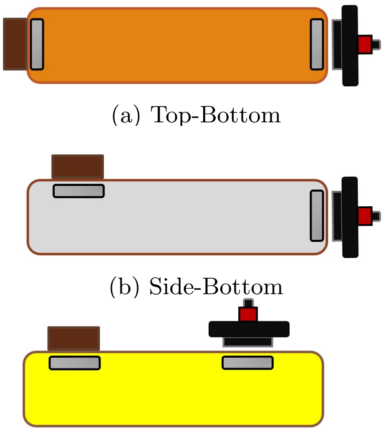

(a) Top-Bottom

(b) Side-Bottom

(c) Side-Side

Fig. 7: Balloon plate designs for different positions of payload and rigid connections.

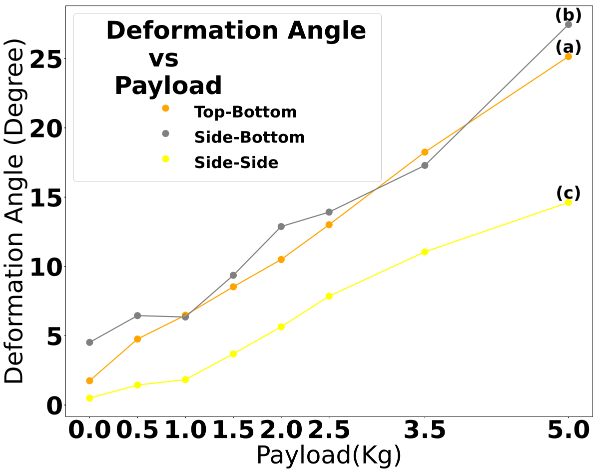


Fig. 8: Deformation Angle in Degree vs Payload in Kg. Comparison of (a) Top-Bottom, (b) Side-Bottom, (c) Side-Side plate orientations for varying payload.

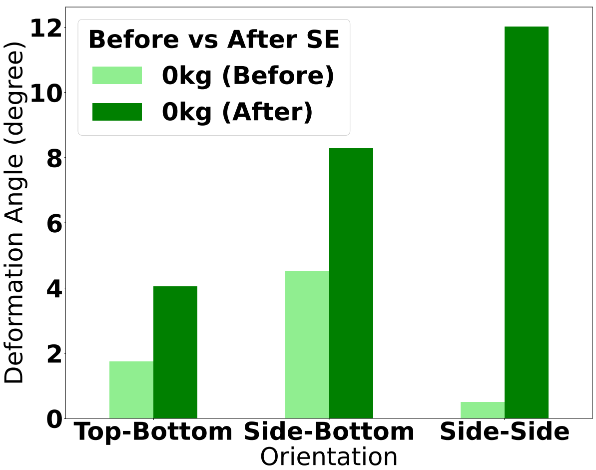


Fig. 9: Comparison of Deformation angle before and after stationary experiment for Top-Bottom, Side-Bottom, Side-Side plate orientations.

### 4·2 Motion Experiment

Motion Experiment is performed in a sinusoidal motion with a frequency of 0.1 [Hz] and amplitude of 45 degrees with the vertical position as the initial posi-

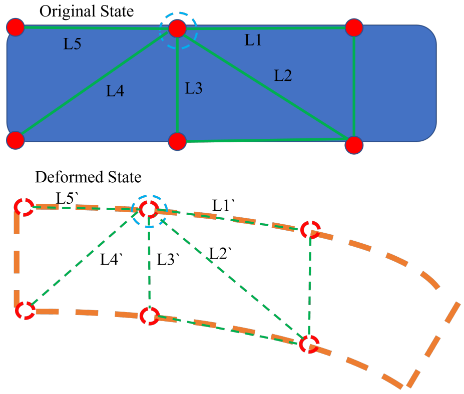


Fig. 10: Measure of deformation index (DI) from original state to deformed state.

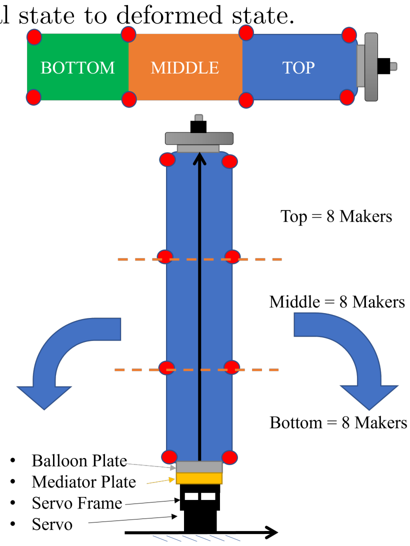


Fig. 11: 1DOF motion experiment setup for motion capture. Red dots represent markers to track inflatable body in real-time.

tion. Weights are used for a payload range from 0kg to 2.5kg. From the stationary experiment, we select the top-bottom plate design to analyze its behavior in motion. The motion experiment utilizes motion capture to track the inflatable link shape in real-time.

We define a deformation metric (Deformation Index (DI)) for each marker position as shown in figure 10. From the equation 1 and the deformed state in figure10, we can observe the deformation index as a summation of change in length divided by the original length across all the markers and normalized by the total number of markers.

$$\mathrm{DI}(L) = \frac{1}{N}\sum_{n=1}^{N}\left(\frac{L_i - L_i'}{L_i}\right) \tag{1}$$

To track the real-time shape of the inflatable link we placed 16 markers as shown in Figure 11. We shall analyze the deformation of 3 parts divided equally as Top, Middle, and Bottom. Each part consists of 8 markers and the deformation index is calculated separately for each of these parts.

Part-wise deformation index indicates the deformation of the Bottom part is bigger than the Top part and the Middle part (refer figure12).

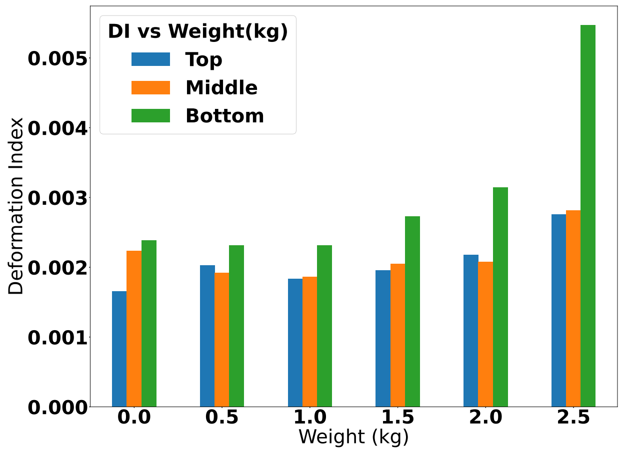


Fig. 12: Comparison of deformation index vs payload (kg) for top, middle and bottom parts of balloon.

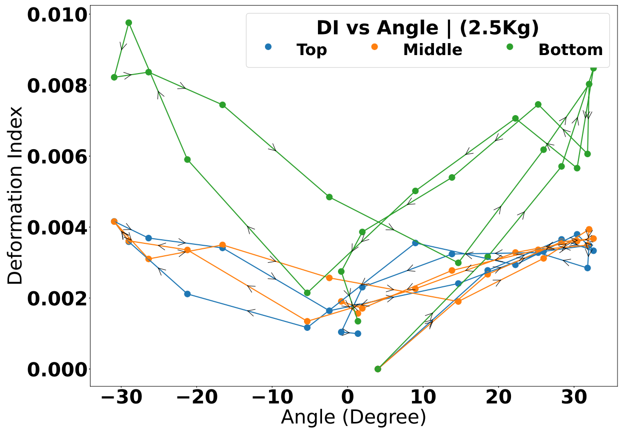


Fig. 13: Comparison of deformation index vs angle(degree) for top, middle and bottom parts of balloon. for 2.5kg.

Figure 13 shows the angle versus deformation index for every 100th frame across the complete sinusoidal motion. The result indicates that the deformation index is highest at both ends of the movement, and it is more visible as the weight increases. The trajectory of the index for the bottom part represents a distorted hysteresis, which can be confirmed from the video included as supplement material.

## 5. 3 Degree of Freedom Robot Design

According to the results of stationary and motion experiments, we can establish the physical properties of 1DOF Inflatable Link. In figure 14 we can see a 2DOF 2 link system. By adding another degree at the base with the help of a Rotary table we can visualize a 3DOF 2 link system. This can be built with inflatable bodies as links as shown in the schematic diagram.

## 6. Conclusion

This paper presents the comparison of Inflatable robot arm joints in different designs. The analysis of data from the experiments confirmed that Top-Bottom plate design is better suited for a 3DOF robot. The bottom part shall experience aging as it sustains maximum deformation and hysteresis confirms its nonlinear behavior.

Multiple-use and aging can lead to Plastic Deformation, hence should be accounted for, in the control protocol. A Deep Learning algorithm as control will be suitable because of its nonlinear properties and the model can be simply retrained without the expert knowledge of fluid dynamics and material properties.

(a) 2DOF 2link

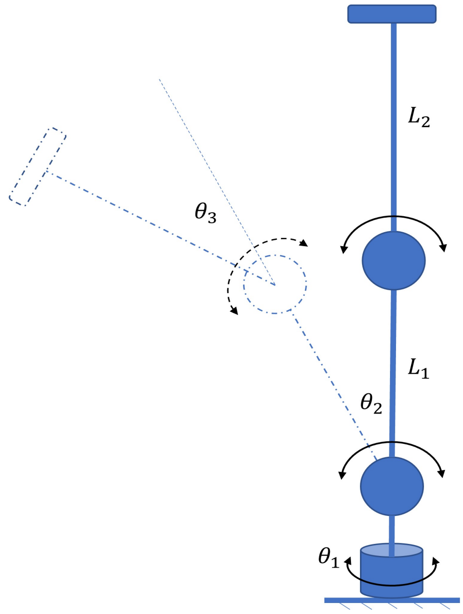


(b) 3DOF 2link

Fig. 14: Realized 2DOF robot arm and visualized the design schematic of 3DOF robot arm.

## References


[1] Daniela Rus and Michael Thomas Tolley. "design, fabrication and control of soft robots". *Nature*, 521:467–475, 2015.

[2] Masashi Takeichi, Koichi Suzumori, Gen Endo, and Hiroyuki Nabae. "development of a 20-m-long giacometti arm with balloon body based on kinematic model with air resistance". In *2017 IEEE/RSJ International Conference on Intelligent Robots and Systems (IROS)*, pages 2710–2716, 2017.

[3] Siddharth Sanan, Peter S. Lynn, and Saul T. Griffith. "pneumatic torsional actuators for inflatable robots". *Journal of Mechanisms and Robotics*, 6:031003, 2014.

[4] Morgan T. Gillespie, Charles M. Best, and Marc D. Killpack. "simultaneous position and stiffness control for an inflatable soft robot". In *2016 IEEE International Conference on Robotics and Automation (ICRA)*, pages 1095–1101, 2016.

[5] Matthias Hofer and Raffaello D'Andrea. "design, fabrication, modeling and control of a fabric-based spherical robotic arm". *Mechatronics*, 68:102369, 2020.

[6] Alexander Alspach, Joohyung Kim, and Katsu Yamane. "design and fabrication of a soft robotic hand and arm system". In *2018 IEEE International Conference on Soft Robotics (RoboSoft)*, pages 369–375, 2018.

[7] Hiroki Sato, Young ah Seong, Ryosuke Yamamura, Hiromasa Hayashi, Katsuhiro Hata, Hisato Ogata, Ryuma Niiyama, and Yoshihiro Kawahara. "soft yet strong inflatable structures for a foldable and portable mobility". *Extended Abstracts of the 2020 CHI Conference on Human Factors in Computing Systems*, 2020.